Self-consistent mode-coupling theory of excitation transport with long-range transfer rates in solution

Daniel S. Franchi, Roger F. Loring, and Shaul Mukamel[a)]
Department of Chemistry, University of Rochester, Rochester, New York 14627

(Received 9 January 1987; accepted 19 February 1987)

A self-consistent mode-coupling theory for incoherent excitation transport is applied to the calculation of excitation dynamics in solution. The long time transport properties for multipolar, $w(r) \sim (\sigma/r)^m$, exchange, $w(r) \sim \exp[-(r-\sigma)/R)]$, and Gaussian, $w(r) \sim \exp[-(r^2-\sigma^2)/\gamma^2]$, transfer rates are compared using the same self-consistent procedure. r is the intermolecular separation, and σ is the molecular hard-sphere diameter. Diffusive behavior is found to hold at long times in all cases. However as the transfer rates become more short range (increasing m and decreasing R and γ), the diffusion coefficient shows an abrupt variation with density, which resembles a percolation transition.

I. INTRODUCTION

We have recently developed a self-consistent mode-coupling (SCMC) theory for incoherent excitation transport in disordered systems.[1] The theory focuses on $D(\mathbf{k},\epsilon)$, the generalized diffusion kernel in Fourier–Laplace space and $P_0(t)$, the configuration-averaged probability that an excitation that resides on a given chromophore at time τ can be found on the same chromophore at a later time $t+\tau$. A pair of coupled equations for these quantities was derived. In Ref. 1, we used the SCMC to calculate transport properties of a disorderd lattice with excitation transfer rates that are nonzero only between molecules occupying nearest-neighbor sites (the site percolation problem). We showed that the SCMC in three dimensions provides an improvement over other theories of incoherent transport in that it is the only formulation that is exact at low densities and in the ordered lattice limit, that predicts a transition in the site percolation problem, that is consistent with the predictions of scaling theories, and that can be applied to transfer rates $w(r)$ with an arbitrary distance dependence. We have further applied the SCMC to the calculation of the vibrational density of modes in disordered lattices.[2] An extension of the SCMC was developed and applied to the quantum percolation problem and to the Anderson localization.[3]

In this article we consider the continuum version of the SCMC and apply it to investigate the transport of excitations in solutions with multipolar, exchange, and Gaussian transfer rates. A formal mathematical analysis shows that a percolation transition[4–6] will occur only if the transfer rate has an upper cutoff [i.e., $w(r)$ vanishes for r greater than some distance r_0].[1,7] For extended-range transfer rates of the type considered here, the motion of excitations will always be diffusive at long times, i.e., $P_0(t) \sim t^{-d/2}$ and the mean-squared displacement of the excitation $<r^2(t)> \sim 2dDt$, in d dimensions.[8] However, if the transfer rates are of sufficiently short range, this behavior will occur at extremely long and unphysical times. For times of physical interest, the system may behave as though there were a percolation transition, with excitations that appear to be localized below a critical value of the chromophore density.

II. THE SELF-CONSISTENT MODE-COUPLING EQUATION FOR EXCITATION TRANSPORT IN SOLUTION

We consider a solution with N solute molecules (chromophores), which can retain and transfer an excitation in a d dimensional volume V. The pair distribution function of the chromophores is denoted $g(r)$,[9] where r is the intermolecular separation. The dynamics of excitations in the system are governed by a Pauli master equation,[1,7,8]

$$\frac{d\mathbf{P}}{dt} = \mathbf{W}\cdot\mathbf{P}, \tag{2.1}$$

where $\mathbf{P}$ is an N-dimensional vector whose nth element is the probability that the excitation resides on the nth chromophore. The $N \times N$ matrix $\mathbf{W}$ has the elements

$$W_{nm} = w_{nm} - \delta_{nm} \sum_j w_{jn}. \tag{2.2}$$

w_{nm} is the rate of excitation transfer between the chromophores labeled n and m, and $w_{nn} = 0$. It is assumed that the chromophores are identical so that $w_{nm} = w_{mn}$.

We wish to calculate $G(\mathbf{r},t)$, the configuration-averaged probability that an excitation will undergo a displacement $\mathbf{r}$ in a time t,

$$G(\mathbf{r},t) = (N-1)\langle \delta(\mathbf{r}-\mathbf{r}_{12})[\exp(\mathbf{W}t)]_{21}\rangle + \langle \delta(\mathbf{r})[\exp(\mathbf{W}t)]_{11}\rangle, \tag{2.3}$$

where the angular brackets denote the configuration average

$$\langle(\cdots)\rangle = V^{-N}\int (\cdots)d\mathbf{r}_1\cdots d\mathbf{r}_N. \tag{2.4}$$

It will be useful to coarse-grain the Green function in Eq. (2.3). To that end we introduce a spatial coarse-graining function $Z(\mathbf{r})$, which is sharply peaked around $\mathbf{r}=0$ and has the normalization

$$\int Z(\mathbf{r})d\mathbf{r} = V_0. \tag{2.5}$$

We then define

[a)] Camille and Henry Dreyfus Teacher–Scholar.

 0021-9606/87/116419-06$02.10

$$P(\mathbf{r},t) = \int G(\mathbf{r}-\mathbf{r}',t)Z(\mathbf{r}')d\mathbf{r}'. \tag{2.6}$$

$P(\mathbf{r},t)$ is the probability to find the excitation at time t in a volume V_0 around $\mathbf{r}$.

We adopt the following definitions of the Fourier and Laplace tranforms for any functions $A(\mathbf{r})$, and $B(t)$:

$$A(\mathbf{k}) = (2\pi)^{-d/2}\int d\mathbf{r}\exp(i\mathbf{k}\cdot\mathbf{r})A(\mathbf{r}), \tag{2.7a}$$

$$B(\epsilon) = \int_0^\infty dt\, B(t)\exp(-\epsilon t). \tag{2.7b}$$

Performing the Fourier and Laplace transforms of Eq. (2.6) results in

$$P(\mathbf{k},\epsilon) = (2\pi)^{-d/2}Z(\mathbf{k})G(\mathbf{k},\epsilon), \tag{2.8}$$

where

$$Z(\mathbf{k}) = (2\pi)^{-d/2}\int d\mathbf{r}\exp(i\mathbf{k}\cdot\mathbf{r})Z(\mathbf{r}), \tag{2.9}$$

and $G(\mathbf{k},\epsilon)$ is the Fourier and Laplace transform of $G(\mathbf{r},t)$. We then write $G(\mathbf{k},\epsilon)$ in terms of a diffusion kernel $D(\mathbf{k},\epsilon)$

$$G(\mathbf{k},\epsilon) = [\epsilon + k^2 D(\mathbf{k},\epsilon)]^{-1}. \tag{2.10}$$

Equations (2.8) and (2.10) result in

$$P(\mathbf{k},\epsilon) = (2\pi)^{-d/2}Z(\mathbf{k})[\epsilon + k^2 D(\mathbf{k},\epsilon)]^{-1}. \tag{2.11}$$

The coarse-grained probability for the excitation to be on the original chromophore is

$$P_0(\epsilon) = \int_0^\infty dt\, P(\mathbf{r}=0,t)\exp(-\epsilon t). \tag{2.12}$$

Our self-consistent mode-coupling procedure consists of two coupled equations for the dynamical quantities $D(\mathbf{k},\epsilon)$ and $P_0(\epsilon)$. One equation is exact and follows directly from Eqs. (2.11) and (2.12):

$$P_0(\epsilon) = \int d\mathbf{k}\, Z(\mathbf{k})[\epsilon + k^2 D(\mathbf{k},\epsilon)]^{-1}. \tag{2.13}$$

In order to derive the second equation, we write $D(\mathbf{k},\epsilon)$ as a functional of $P_0(\epsilon)$ that depends on ϵ only through its dependence on $P_0(\epsilon)$:

$$D(\mathbf{k},\epsilon) = \tilde{D}[\mathbf{k},P_0(\epsilon)]. \tag{2.14}$$

Equation (2.14) should be regarded as a definition of the functional $\tilde{D}$. The justification of this definition is discussed in Ref. 1. $\tilde{D}$ depends explicitly on the chromophore density, and also depends implicitly on this density through the density dependence of P_0. In Ref. 1, we demonstrated that $\tilde{D}$ can be calculated order-by-order in an expansion with respect to its explicit density dependence. The terms in this expansion can be determined from a knowledge of the density expansions of $P_0(\epsilon)$ and $D(\mathbf{k},\epsilon)$. The first term in this resummed density expansion is[1,7]

$$\tilde{D}(\mathbf{k},P_0) = k^{-2}(c/\sigma^d)\int \{w(\mathbf{r})/[1+2w(\mathbf{r})P_0]\}[1-\exp(i\mathbf{k}\cdot\mathbf{r})]g(\mathbf{r})d\mathbf{r}, \tag{2.15}$$

where we have introduced the dimensionless density of chromophores c,

$$c = \frac{N\sigma^d}{V}. \tag{2.16}$$

For a spherically symmetric system in which $w(\mathbf{r})$ and $g(\mathbf{r})$ are functions only of $|\mathbf{r}|$, the angular integrals in Eqs. (2.13) and (2.15) can be performed to yield our final SCMC equation:

$$P_0(\epsilon) = \Omega_d\int_0^\infty Z(k)[\epsilon + k^2\tilde{D}(k,P_0)]^{-1}k^{d-1}dk, \tag{2.17a}$$

$$k^2\tilde{D}(k,P_0) = \Omega_d(c/\sigma^d)\int_0^\infty \{w(r)/[1+2w(r)P_0]\}\times[1-\sin(kr)/(kr)]g(r)r^{d-1}dr. \tag{2.17b}$$

$\Omega_d = d\pi^{d/2}/[(d/2)!]$ is the solid angle in d dimensions. Equations (2.17a) and (2.17b) are the continuum analogs of Eqs. (2.14) of Ref. 1, which were derived for excitation transport on a lattice.

III. APPLICATION TO LONG-RANGE TRANSFER RATES

We shall now use the SCMC equation [Eqs. (2.17a) and (2.17b)] to examine the influence of the distance dependence of the transfer rate $w(r)$ on the transport of excitations in solution in three dimensions. The pair distribution function of the chromophores is taken to be[9]

$$g(r) = \begin{cases} 0 & r<\sigma \\ 1 & r\geqslant\sigma \end{cases}, \tag{3.1}$$

σ is the molecular diameter. Substituting Eq. (3.1) into Eqs. (2.17) and setting $d=3$ yields

$$P_0(\epsilon) = 4\pi\int_0^\infty Z(k)[\epsilon + k^2\tilde{D}(k,P_0)]^{-1}k^2dk, \tag{3.2a}$$

$$k^2\tilde{D}(k,P_0) = 4\pi w_0(c/\sigma^3)\int_\sigma^\infty [1-(\sin kr)/(kr)]\times[w_0/w(r)+2w_0P_0]^{-1}r^2dr. \tag{3.2b}$$

$w_0 \equiv w(\sigma)$ denotes the transfer rate at contact. We shall consider transfer rates with the following functional forms:

$$w(r) = w_0(\sigma/r)^m, \tag{3.3}$$

$$w(r) = w_0\exp[-(r-\sigma)/R], \tag{3.4}$$

$$w(r) = w_0\exp[-(r^2-\sigma^2)/\gamma^2]. \tag{3.5}$$

Excitation transfer arising from multipolar interactions is governed by a rate of the form given in Eq. (3.3), where m is an integer greater than or equal to 6. For $m=6$, Eq. (3.3) gives the Förster dipole–dipole transfer rate.[10–13] Excitation transfer caused by exchange interactions, such as the transfer of a triplet excitation, is described by the exponential form of Eq. (3.4). A rate of this form is also used to describe electron transfer.[14]

In order to compare quantitatively the transport properties for rates (3.3)–(3.5), we introduce the integrated transfer rate S:

$$S = (w_0\sigma^3)^{-1}\int_\sigma^\infty w(r)r^2dr. \tag{3.6}$$

For $w(r)$ given by Eqs. (3.3), (3.4), (3.5), S is given by Eqs. (3.7a), (3.7b), (3.7c), respectively:

$$S = 1/(m-3), \tag{3.7a}$$

$$S = R/\sigma + 2(R/\sigma)^2 + 2(R/\sigma)^3, \tag{3.7b}$$

$$S = (\gamma/\sigma)^2/2 + [(\gamma/\sigma)^3/2](\pi^{1/2}/2)$$

$$\times\{\exp[(\sigma/\gamma)^2] - \mathrm{erf}(\sigma/\gamma)\}, \tag{3.7c}$$

where erf denotes the error function.[15] In the calculations presented in Sec. IV, we shall compare the transport properties for rates (3.3)–(3.5), and we shall choose m, R, and γ such that the integrated transfer rate S is the same for each model.

Transport properties can be calculated from Eqs. (3.2) as follows. Substitution of Eq. (3.2b) into Eq. (3.2a) yields a closed equation for $P_0(\epsilon)$, which can be solved numerically,[16] for given value of c. The Laplace transform can be inverted numerically[17] to yield $P_0(t)$. Substitution of $P_0(\epsilon)$ into the right-hand side of Eq. (3.2b) gives $D(k,\epsilon)$, from which the propagator $P(k,\epsilon)$ can be determined, according to Eq. (2.11). The time-dependent mean-squared displacement of an excitation is defined by

$$\langle r^2(t)\rangle = \int d\mathbf{r}\, r^2 P(\mathbf{r},t). \tag{3.8}$$

According to Eqs. (2.11), (2.15), (3.2), and (3.8), the Laplace transform of the mean-squared displacement $\langle r^2(\epsilon)\rangle$ in three dimensions is

$$\langle r^2(\epsilon)\rangle = (6/\epsilon^2)\tilde{D}[0,P_0(\epsilon)], \tag{3.9a}$$

where

$$\tilde{D}(0,P_0) = (2\pi/3)w_0(c/\sigma^3) \times \int_\sigma^\infty [w_0/w(r) + 2w_0P_0]^{-1} r^4 dr. \tag{3.9b}$$

The behavior of $\langle r^2(t)\rangle$ at long times can be deduced from Eq. (3.9a) with the use of the Tauberian theorem for Laplace transforms.[18] If $\tilde{D}[0,P_0(\epsilon)]$ approaches a finite limit as $\epsilon\to 0$, then $\langle r^2(t)\rangle$ will increase linearly in time at long times:

$$\langle r^2(t)\rangle \sim 6Dt, \qquad t\to\infty, \tag{3.10a}$$

$$D = \lim_{\epsilon\to 0} \tilde{D}\,[0,P_0(\epsilon)]. \tag{3.10b}$$

In Ref. 1, we showed that for any transfer rate without an upper cutoff, the SCMC equation predicts the following asymptotic, long-time behavior of $\langle r^2(t)\rangle$ and $P_0(t)$ in d dimensions,

$$\langle r^2(t)\rangle \sim t, \tag{3.11a}$$

$$P_0(t) \sim t^{-d/2}. \tag{3.11b}$$

Equations (3.11a) and (3.11b) are also predicted by a scaling argument, which is based on the assumption that at long times there is a single relevant length scale in the problem. This assumption will not hold if the transfer rate has an upper cutoff (e.g., the percolation problem), but it is expected to be valid for any rate without such a cutoff. The behavior of $\langle r^2(t)\rangle$ and $P_0(t)$ at long times, calculated from Eqs. (3.2) for each of the transfer rates in Eqs. (3.3)–(3.5) is thus given by Eqs. (3.11a) and (3.11b). However, such asymptotic analysis does not tell us how long we must wait for the limits of Eqs. (3.11a) and (3.11b) to be attained. In order to calculate the transport for all times and to determine *when* it becomes diffusive, we must solve Eqs. (3.2) numerically. This is done in the following section.

IV. CALCULATION OF TRANSPORT PROPERTIES

We shall now present the solution of the SCMC equation [Eqs. (3.2)] at all times for the transfer rates [Eqs. (3.3)–(3.5)]. In all the calculations we have taken $\sigma = 1$. In Fig. 1 we display the time-dependent probability for the excitation to be on the initially excited chromophore, $P_0(t)$, for the dipolar transfer rate [Eq. (3.3) with m = 6]. For the coarse-graining function we have used

$$Z(k) = \begin{cases} 3\sigma^3/(4\pi^4) & k\leqslant \pi/\sigma \\ 0 & k>\pi/\sigma \end{cases}, \tag{4.1}$$

so that $V_0 = 0.2316(\pi\sigma^3/6)$. We shall denote the closest packing value of c by $c^* = 2^{1/2}$. This corresponds to a face-centered cubic or hexagonal close-packed lattice.[5] The solid curves in Fig. 1 correspond to $c/c^* = 0.01$, 0.1, 0.3, and 0.9 as indicated. The slope of the dash–dot curve represents a $t^{-3/2}$ behavior. In all cases, the long time behavior of $\sim t^{-3/2}$ is attained as expected.[1] As the density is increased, the asymptotic behavior is attained at shorter times. For comparison, we display $P_0(t)$ calculated using a first-order cumulant in density.[7] These calculations are given by the dashed curves in Fig. 1. The first order cumulant approximation for $P_0(t)$ is[7]

$$P_0(t) = \exp\left[-(c/\sigma^3)\int\{1-\exp[-2w(\mathbf{r})t]\}g(\mathbf{r})d\mathbf{r}\right]. \tag{4.2}$$

Substituting in the dipole–dipole transfer rate and Eq. (3.1) into Eq. (4.2) yields

$$P_0(t) = \exp(-c(2\pi/3)\{(\pi 2w_0t)^{1/2}\,\mathrm{erf}[(2w_0t)^{1/2}] - [1-\exp(-2w_0t)]\}). \tag{4.3}$$

For long times, Eq. (4.3) assumes the form

$$P_0(t) = \exp(-At^{1/2}) \tag{4.4a}$$

with

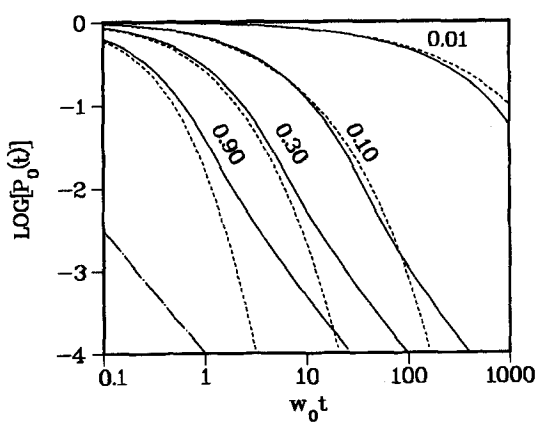

FIG. 1. $P_0(t)$, the probability that an excitation will be found on the initially excited chromophore after a time t, for the dipole–dipole transfer rate [Eq. (3.3) with $m = 6$]. The solid lines represent the solution of the SCMC equation [Eqs. (3.2)] for $c/c^* = 0.01$, 0.10, 0.30, 0.90, as indicated. $\sigma = 1$. The dashed lines represent the corresponding calculation using the first-order cumulant approximation [Eq. (4.3)]. The plot is given on a logarithmic scale (base 10) and the dot–dashed line represents a $t^{-3/2}$ behavior.

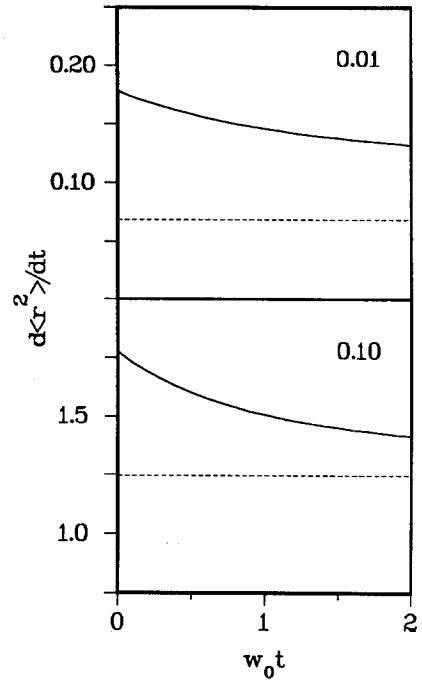

FIG. 2. The time derivative of the mean-squared displacement [Eq. (3.8)], for the $c/c^* = 0.01$ and 0.10. The dashed lines represent the asymptotic diffusion coefficient $6D$ [Eq. (3.10a)].

$$A = \frac{2\pi}{3} c (2\pi w_0)^{1/2}. \tag{4.4b}$$

The cumulant approximation is not self-consistent and $P_0(t)$ is insensitive to the dimensionality d. At long times, it fails to reproduce the $t^{-3/2}$ behavior. The dashed curves in Fig. 1 demonstrate that the cumulant approximation always agrees with the SCMC at short times but that at large times it decays much faster than the SCMC.

The solid curves in Fig. 2 and Fig. 3 represent the time derivative of the mean-squared displacement [Eq. (3.10)] for the dipole–dipole transfer rate [Eq. (3.3) with $m = 6$] for the same values of c/c^* used in Fig. 1. The long-time limits of these curves is $6D$ [Eq. (3.10a)], and is indicated by the dashed curves. As in Fig. 1, the plots demonstrate the time scale in which the asymptotic behavior is attained. This time scale is shorter for higher densities.[19]

We shall now explore the dependence of the long-time transport properties on the functional form of the transfer rate $w(r)$. We have solved the SCMC equation [Eqs. (3.2)] using the multipolar Eq. (3.3), the exponential Eq. (3.4), and the Gaussian Eq. (3.5) transfer rates. In each case we have calculated the diffusion coefficient D [Eq. (3.10b)]. To simplify the numerical calculations, we have used in Figs. 4–7 a Gaussian coarse-graining function,

$$Z(r) = (2\pi)^{-3/2} \exp(-r^2/a^2). \tag{4.5a}$$

The Fourier transform $Z(k)$, as defined by Eq. (2.9), is

$$Z(k) = (a/2\pi^{1/2})^3 \exp(-k^2 a^2/4). \tag{4.5b}$$

We have taken $\sigma = 1$ and $a = 0.09$. The diffusion coefficient for a perfect crystal with closest packing ($c = c^*$) and with nearest neighbor interactions is given by[1]

$$\bar{D} = (2^{3/2}\pi/3) w_0 \sigma^2. \tag{4.6a}$$

We shall introduce the dimensionless diffusion coefficient

$$D_0 \equiv D/\bar{D}. \tag{4.6b}$$

The solid lines in Fig. 4 show D_0 vs c/c^* for the multipolar

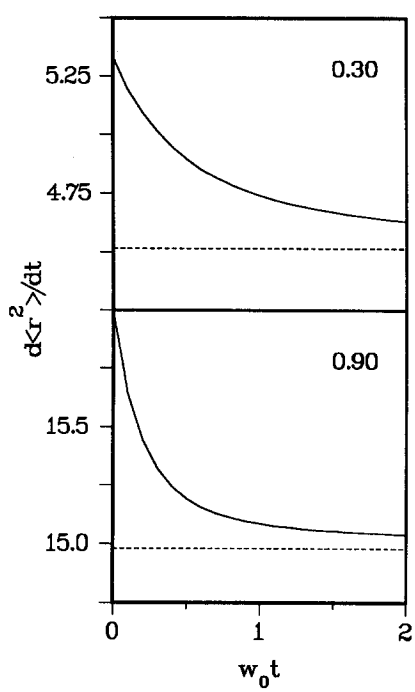

FIG. 3. Same as Fig. 2 for $c/c^* = 0.30$ and 0.90.

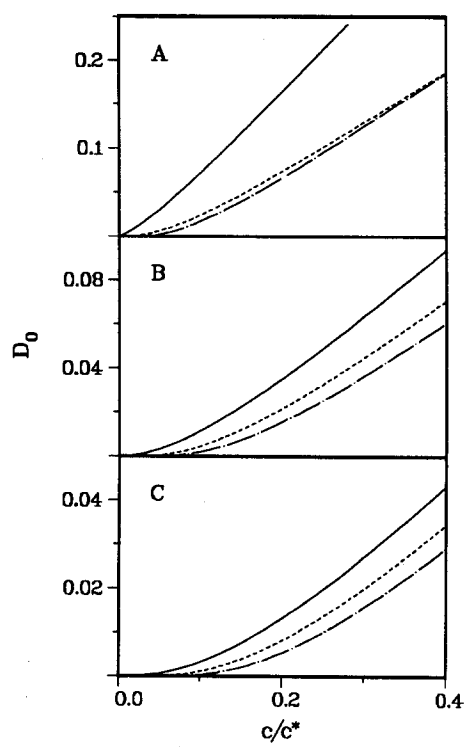

FIG. 4. The dimensionless diffusion coefficient D_0 [Eqs. (4.6)] obtained from the SCMC equation [Eqs. (3.2)] vs density. The solid lines correspond to the multipolar rate with $m = 6$ (A), $m = 8$ (B), and $m = 10$ (C). In each panel, we also display D_0 for the exponential (dashed curves) and Gaussian (dash–dot curves) transfer rates, with the same value of the integrated transfer rate S [Eqs. (3.7)].

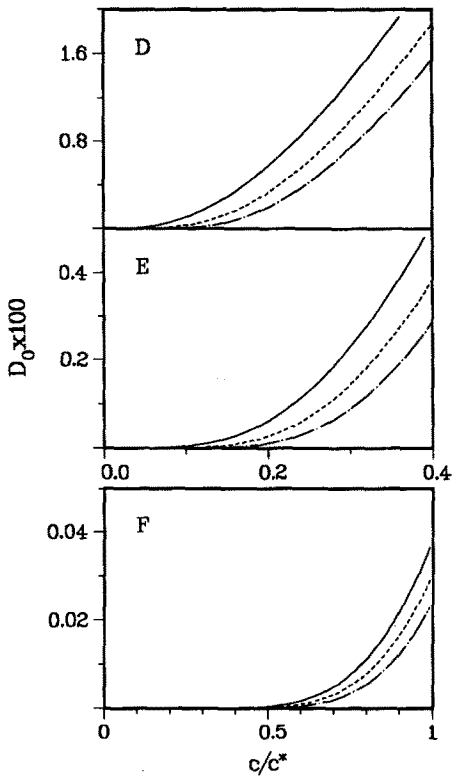

FIG. 5. The same as Fig. 4 but for higher values of m (smaller values of S) $m = 12$ (D), $m = 18$ (E) and $m = 60$ (F).

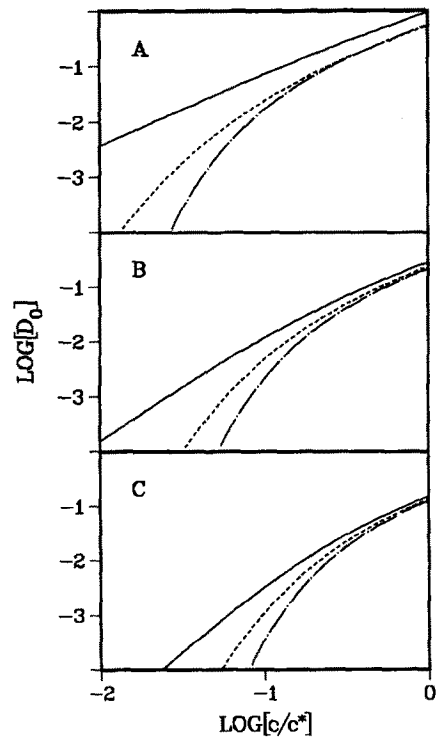

FIG. 6. The same as Fig. 4 plotted on a logarithmic scale (base 10).

rate [Eq. (3.3)]. Panels A, B, and C correspond to $m = 6$, 8, and 10, respectively. In each panel, we also display D_0 for the exponential [Eq. (3.4), dashed curves] and the Gaussian [Eq. (3.5), dash–dot curves] transfer rates with the same value of the integrated transfer rate S [Eqs. (3.7)]. In Fig. 5 we show the same comparison for $m = 12$ (panel D), $m = 19$ (panel E), and $m = 60$ (panel F). The calculations demonstrate that D_0 is finite for any value of c, and that the long-time behavior is always diffusive [Eqs. (3.11)]. However, the diffusion coefficient can show an abrupt change with density. This change becomes sharper as the transfer rate becomes more short range (S decreases), and it resembles the percolation transition. For a given value of S, all three transfer rates have the same qualitative behavior, although the abrupt transition becomes sharper as we go from the multipolar to the exponential and to the Gaussian transfer rate.

Phillips has recently argued[20] that transport properties for exponential and Gaussian transfer rates in three dimensions at long times should be qualitatively different. His arguments indicate that an exponential transfer rate will always result in diffusive transport whereas a Gaussian rate may lead to localization and the absence of diffusion (percolation). Our analysis and the calculations shown in Figs. 4 and 5 do not support these arguments. We find no qualitative difference between the three transfer rates for a given value of the integrated transfer rate S.

In order to display the diffusion coefficient D_0 for small c more clearly, we have replotted D_0 of Figs. 4 and 5 in Figs. 6 and 7 on a logarithmic scale. Scaling arguments introduced by Haan and Zwanzig[11] show that for the multipolar rate, D_0 should scale as $\sim c^{(m-2)/3}$ for small c. This results from the assumption that the long-time behavior is dominated by a single length scale. This assumption allows us to write the diffusion coefficient in the form

$$D(c,0,\epsilon) = \epsilon^{(m-2)/m} D(\epsilon^{-3/m} c,0,1). \tag{4.7}$$

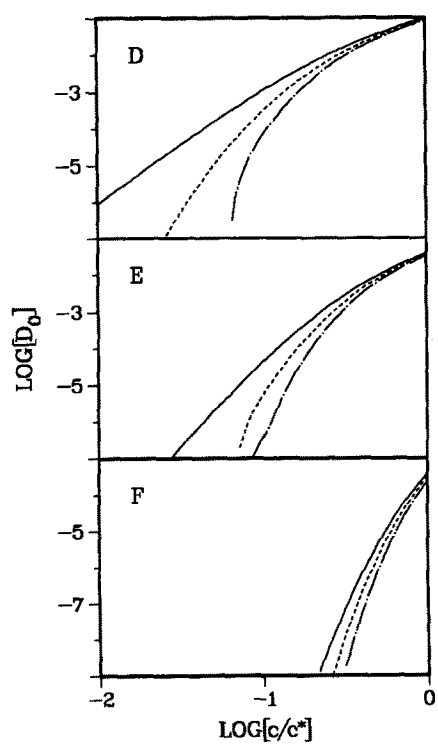

FIG. 7. The same as Fig. 5 plotted on a logarithmic scale (base 10).

The existence of an ordinary diffusion coefficient (independent of ϵ), then implies that D should scale as $c^{(m-2)/3}$. At higher densities, the hard-sphere diameter σ provides another length scale and the dependence of D_0 on c no longer follows this simple behavior. The solid lines in Figs. 6 and 7 all start as $c^{(m-2)/3}$ at low densities in accordance with this scaling argument.

ACKNOWLEDGMENTS

The support of the National Science Foundation, the Office of Naval Research, the U.S. Army Research Office, and of the donors of the Petroleum Research Fund, administered by the American Chemical Society, is gratefully acknowledged.

[1]R. F. Loring, D. S. Franchi, and S. Mukamel, J. Chem. Phys. **86**, 1323 (1987).
[2]R. F. Loring and S. Mukamel, Phys. Rev. B **34**, 6582 (1986).
[3]R. F. Loring and S. Mukamel, Phys. Rev. B **33**, 7708 (1986); J. Chem. Phys. **85**, 1950 (1986); R. F. Loring, M. Sparpaglione, and S. Mukamel, *ibid.* **86**, 2249 (1987).
[4]D. Stauffer, Phys. Rep. **54**, 1 (1979); *Introduction to Percolation* (Taylor and Francis, Philadelphia, 1985).
[5]R. Zallen, *The Physics of Amorphous Solids* (Wiley, New York, 1983).
[6]*Percolation Structure and Processes*, edited by G. Deutscher, R. Zallen, and J. Adler, Annals of the Israel Physical Society (Adam Hilger, Bristol, England, 1983), Vol. 5.
[7]J. Nieuwoudt and S. Mukamel, Phys. Rev. B **30**, 4426 (1984); J. Stat. Phys. **36**, 677 (1984).
[8]S. Alexander, J. Bernasconi, W. Schneider and R. Orbach, Rev. Mod. Phys. **53**, 175 (1981).
[9]J. P. Hansen and I. R. MacDonald, *Theory of Simple Liquids* (Academic, New York, 1976).
[10]T. Förster, Ann. Phys. (Leipzig) **2**, 55 (1948).
[11]S. W. Haan and R. Zwanzig, J. Chem. Phys. **68**, 1879 (1978).
[12]P. A. Anfinrud, D. E. Hart, J. F. Hedstrom, and W. S. Struve, J. Chem. Phys. **90**, 2374, 3116 (1986).
[13]L. Gomez-Jahn, J. Kasinski, and R. J. D. Miller, Chem. Phys. Lett. **125**, 500 (1986).
[14]D. L. Dexter, J. Chem. Phys. **21**, 836 (1953).
[15]M. Abramowitz and I. A. Stegun, *Handbook of Mathematical Functions* (National Bureau of Standards, 1972), p. 297.
[16]G. E. Forsythe, M. A. Malcolm, and C. B. Moler, *Computer Methods for Mathematical Computations* (Prentice–Hall, Englewood Cliffs, New Jersey, 1977), p. 161; J. R. Rice, *Numerical Methods, Software, and Analysis: IMSL Reference Edition* (McGraw–Hill, New York, 1983), p. 243.
[17]H. Stehfest, Commun. ACM **13**, 47, 624 (1970).
[18]G. H. Hardy, *Divergent Series* (Oxford University, Oxford, 1949).
[19]R. F. Loring, H. C. Andersen, and M. D. Fayer, J. Chem. Phys. **80**, 5731 (1984); C. R. Gochanour, H. C. Andersen, and M. D. Fayer, *ibid.* **70**, 4254 (1979).
[20]P. Phillips, J. Chem. Phys. **84**, 976 (1986).